Synthesis, Structure, and Properties of a Novel Metallic Nickel(III) Oxide in the $Ce_{2-x}Sr_xNiO_{4-\delta}$ System: $CeSr_7Ni_4O_{15}$

M. James[†,‡] and J. P. Attfield[*,†]

Department of Chemistry, University of Cambridge, Lensfield Road, Cambridge, CB2 1EW, U.K., and the Interdisciplinary Research Centre in Superconductivity, University of Cambridge, Madingley Road, Cambridge, CB3 0HE, U.K.

Received June 26, 1995. Revised Manuscript Received September 18, 1995[⊗]

The first quaternary cerium strontium nickel oxide, $CeSr_7Ni_4O_{15}$, corresponding to the $x = 1.75$ composition in the $Ce_{2-x}Sr_xNiO_{4-\delta}$ system has been prepared. Thermogravimetric analysis confirms that Ce(IV) and Ni(III) are present. Rietveld refinement using powder X-ray diffraction data indicates a tetragonal K_2NiF_4 type structure ($Z = {}^1/_2$, $a = 3.7999(1)$ Å, $c = 12.3630(2)$ Å, space group $I4/mmm$), with Ce^{4+} and Sr^{2+} disordered over the K sites. Magnetic susceptibility data show Curie−Weiss behavior in the range 6−300 K with a low value of the effective magnetic moment (0.50 μ_B per Ni^{3+} ion). Electrical resistivity measurements demonstrate that $CeSr_7Ni_4O_{15}$ is a metallic conductor although the related phase $YSr_5Ni_3O_{11}$ is semiconducting.

Introduction

Recently there has been a great deal of interest in rare earth nickel oxide phases having the K_2NiF_4 structure (Figure 1) which show structural, magnetic, and electrical similarities to high-T_c copper oxide materials. In particular, the properties of $Ln_{2-x}Sr_xNiO_{4-\delta}$ solid solutions have been extensively studied for Ln = La,[1−3] Nd,[4−6] Pr, Sm, and Gd.[6,7] A range of solid solution up to $x = 1.67$ is found for these early lanthanides,[6] whereas Ln = Y[8,9] and Dy−Tm[9] form essentially point phases at this composition, $Ln_{0.33}Sr_{1.67}NiO_{3.67}$, equivalent to the stoichiometry $LnSr_5Ni_3O_{11}$.

The model proposed for the $LnSr_5Ni_3O_{11}$ phases[8,9] associates one oxygen vacancy with each lanthanide ion in order to reduce the average size of the coordination sphere giving the ideal composition $Ln_{2-x}Sr_xNiO_{2+x}$. The value of x is controlled by the nickel oxidation state in order to maintain charge neutrality. Synthesis of these phases under 1 bar of O_2 leads to a nickel oxidation state of +3 and thus a value of $x = 1.67$. This vacancy model has been supported by Y and Sr K edge EXAFS studies of $YSr_5Ni_3O_{11}$.[9] Another test of this model would be to prepare $Ln_{2-x}Sr_xNiO_{4-\delta}$ phases containing nontrivalent Ln ions. Ce^{4+} is stable under these preparation conditions, comparable in size to the later Ln^{3+} ions, and is predicted to form a phase with $x = 1.75$ by the above model, equivalent to the stoichiometry $CeSr_7Ni_4O_{15}$.

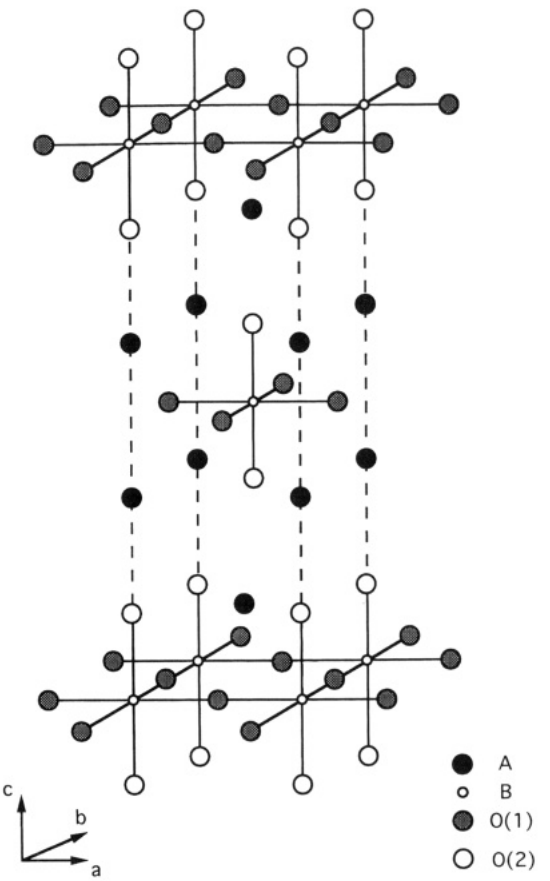

Figure 1. Crystal structure of A_2BO_4 with the tetragonal K_2NiF_4 structure type.

[†] Department of Chemistry, University of Cambridge, Lensfield Road, Cambridge, CB2 1EW, U.K., and Interdisciplinary Research Centre in Superconductivity, University of Cambridge, Madingley Road, Cambridge, CB3 0HE, U.K.

[‡] New address: ANSTO, Lucas Heights Research Laboratories, Private Mail Bag 1, Menai, N.S.W. 2234, Australia.

[*] To whom correspondence is to be addressed.

[⊗] Abstract published in *Advance ACS Abstracts,* November 1, 1995.

(1) Gopalakrishnan, J.; Colsmann, G.; Reuter, B. *J. Solid State Chem.* **1977**, *22*, 145.

(2) Takeda, Y.; Kanno, R.; Sakano, M.; Yamamoto, O.; Takano, M.; Bando, Y.; Akinaga, H.; Takita; K.; Goodenough, J. B. *Mater. Res. Bull.* **1990**, *25*, 293.

(3) Sreedhar, K.; Rao, C. N. *Mater. Res. Bull.* **1990**, *25*, 1235.

(4) Arbuckle, B. W.; Ramanujachary, K. V.; Zhang, Z.; Greenblatt, M. *J. Solid State Chem.* **1990**, *88*, 278.

(5) Takeda, Y.; Nishijima, M.; Imanishi, N.; Kanno, R.; Yamamoto, O.; Takano, M. *J. Solid State Chem.* **1992**, *96*, 72.

(6) James, M.; Attfield J. P. *J. Mater. Chem.*, in press.

(7) Chen, S. C.; Ramanujachary, K. V.; Greenblatt, M. *J. Solid State Chem.* **1993**, *105*, 444.

(8) James, M.; Attfield, J. P. *J. Solid State Chem.* **1993**, *105*, 287.

(9) James, M.; Attfield, J. P.; Rodriguez-Carvajal, *Chem. Mater.* **1995**, *7*, 1448.

0897-4756/95/2807-2338$09.00/0

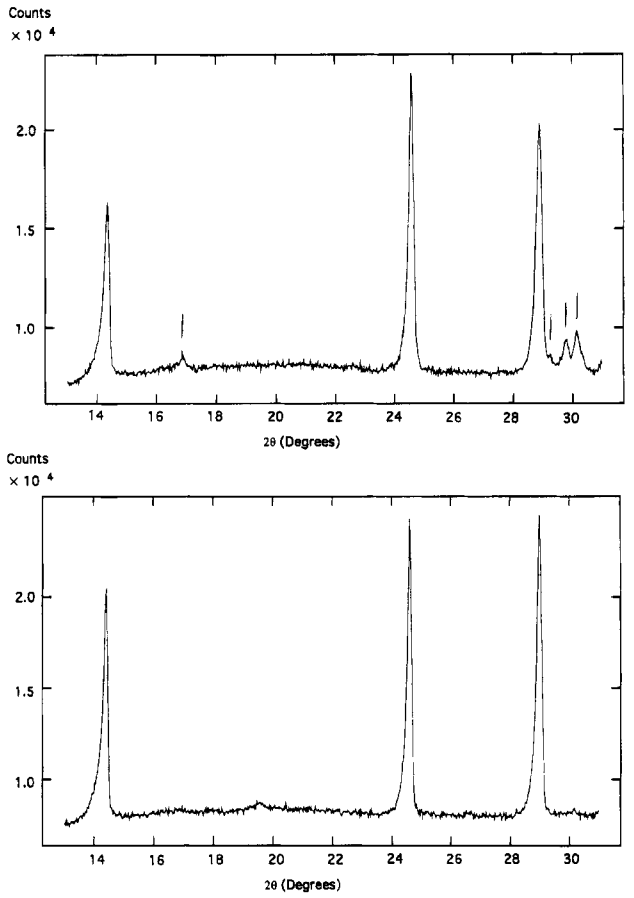

Figure 2. Powder X-ray diffraction patterns ($13 \leq 2\theta \leq 31°$) of nominal compositions (a) $CeSr_5Ni_3O_{11}$ and (b) $CeSr_7Ni_4O_{15}$. Peaks from Sr_2CeO_4 are marked in (a).

This paper describes an attempt to prepare this composition as well as the $x = 1.67$ phase $CeSr_5Ni_3O_{11}$.

Experimental Section

Sample Preparation. Polycrystalline samples with bulk compositions $CeSr_5Ni_3O_{11}$ and $CeSr_7Ni_4O_{15}$ were synthesized from spectroscopic grade powders of strontium carbonate, nickel nitrate hexahydrate, and cerium(III) nitrate hexahydrate. The powders were dissolved in dilute nitric acid, and an intimate mixture of the metal oxides was formed via the decomposition of a citric acid/ethylene glycol gel. The residues were pelleted and sintered in a tube furnace at 1100 °C under flowing oxygen with frequent regrinding and repelleting until no further reaction was evident by powder X-ray diffraction.

Powder Diffraction. Powder X-ray diffraction profiles were recorded on a Philips PW1710 diffractometer, utilizing Cu Kα radiation. Data of sufficient quality for structural refinement were collected over $13° \leq 2\Theta \leq 113°$, in 0.025° steps, with integration times of 12 s. These structural refinements were carried out by the Rietveld method[10] using the GSAS program[11] and a refined background function.

Thermogravimetric Analysis. Thermogravimetric analysis of a ~30 mg sample was carried out using a Stanton Redcroft STA 1500 simultaneous thermal analyzer. The sample was reduced under a 5% hydrogen in nitrogen mixture (flow rate of 58 mL/min) over the temperature range 15–900 °C at a heating rate of 10 °C/min.

Magnetic Susceptibility Measurements. Magnetic susceptibilities were measured using a Quantum Design SQUID magnetometer under an applied field of 3.0 T. The sample was cooled to 6 K in zero field, and the magnetization was measured while warming to 300 K.

Resistivity Measurements. Resistivity measurements were carried out on a sintered pellet in a standard helium cooled Oxford Instruments CF1200 flow cryostat using the the van der Pauw method[12] while warming the sample from 5 to 290 K.

Table 1. Observed *d* Spacings and Relative Peak Heights from the Powder X-ray Diffraction Pattern of $CeSr_7Ni_4O_{15}$

(*hkl*)	*d* spacing (Å)	rel intensity	(*hkl*)	*d* spacing (Å)	rel intensity
002	6.161	6	202	1.812	1
101	3.617	11	211	1.680	2
004	3.087	9	116	1.634	9
103	2.788	100	204	1.616	5
110	2.679	72	107	1.601	5
112	2.458	2	213	1.568	27
105	2.070	17	008	1.545	3
006	2.058	9	215	1.399	8
114	2.025	28	206	1.395	12
200	1.896	32	220/118	1.341	8

Table 2. Results of the X-ray Rietveld Refinement of the Structure of $Ce_{0.25}Sr_{1.75}NiO_{3.75}$ ($CeSr_7Ni_4O_{15}$) in Space Group I4/*mmm*, with Esd's in Parentheses

cell parameters (Å)	$a = 3.7999(1)$	$c = 12.3630(2)$	
R factors (%)	$R_{WP} = 4.6$	$R_P = 2.8$	$R_F = 3.4$

Atomic Parameters

atom	sym position	x	y	z	U_{iso} (Å^2)	occupancy
Ni	(2*a*)	0	0	0	0.0070(7)	1.0
Ce/Sr	(4*e*)	0	0	0.3599(1)	0.0060(3)	0.125/0.875
O(1)	(4*c*)	1/2	0	0	0.010(1)	0.875
O(2)	(4*e*)	0	0	0.1618(4)	0.010	1.0

Interatomic Distances (Å)

Ni–O(1) (×3½)	1.900(1)
Ni–O(2) (×2)	2.001(5)
Ce/Sr–O(1) (×3½)	2.571(1)
Ce/Sr–O(2) (×1)	2.449(5)
Ce/Sr–O(2) (×4)	2.700(1)

Results

Powder X-ray diffraction showed that both the $x = 1.67$ ($CeSr_5Ni_3O_{11}$) and $x = 1.75$ ($CeSr_7Ni_4O_{15}$) samples contained tetragonal K_2NiF_4 type phases. Careful inspection revealed a small amount of the secondary phase Sr_2CeO_4 in the $x = 1.67$ sample while the $x = 1.75$ sample was found to be monophasic (Figure 2). The observed *d* spacings and intensities for $CeSr_7Ni_4O_{15}$ are given in Table 1.

The structures of the two K_2NiF_4 type phases were Rietveld refined in space group I4/*mmm* with Ce and Sr disordered over the K-sites. A good fit was obtained using a pseudo-Voigt peak-shape function. Free refinement of the O(1) and O(2) occupancies for the $x = 1.75$ sample gave values of 0.96(1) and 1.01(1), respectively, that were highly correlated (>70%) with the temperature factors, and so the occupancies were fixed to give the ideal oxygen stoichiometry with all the vacancies located at the O(1) site. This is consistent with previous structural studies of the phases $LnSr_5Ni_3O_{11}$ (Ln = Y,[8,9] Dy, Ho, Er, Tm[9]) which have indicated that oxygen vacancies are present principally at the O(1) sites in the NiO_2 planes. This gave only marginal increases of <0.1% in the profile *R* factors. The results of the

(10) Rieveld, H. M. *J. Appl. Cryst.* **1969**, *2*, 65.
(11) Larson, A. C.; Von Dreele, R. B. Los Alamos National Laboratory Report, No. LA-UR-86-748, **1987**.
(12) Van der Pauw, L. J. *Philips Res. Rep.* **1958**, *13*, 1.
(13) Shannon, R. D. *Acta Crystallogr.* **1976**, *A32*, 751.

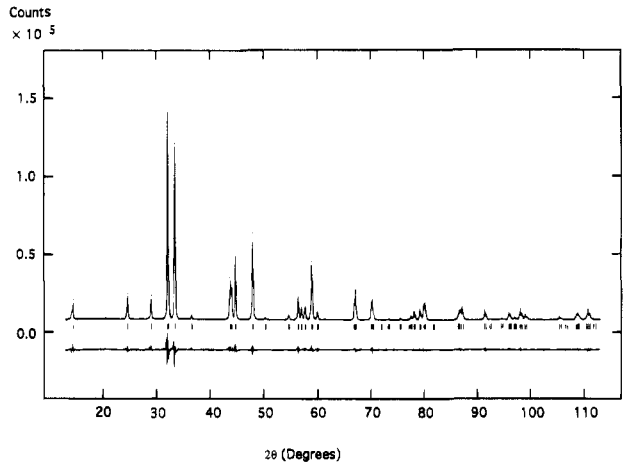

Figure 3. Observed (points), calculated (full line), and difference X-ray powder diffraction patterns for $CeSr_7Ni_4O_{15}$.

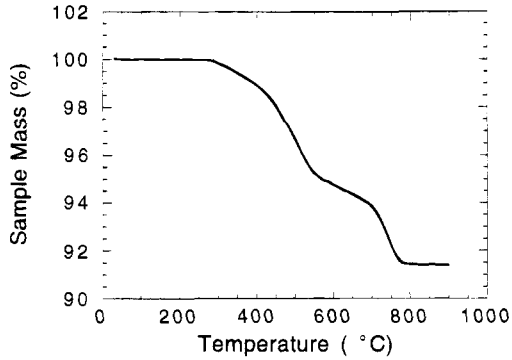

Figure 4. Thermogravimetric reduction profile for $CeSr_7Ni_4O_{15}$.

refinement for the $x = 1.75$ sample are given in Table 2 and the X-ray profiles are shown in Figure 3. The refined parameters from the multiphase $x = 1.67$ sample are almost identical with those of the $x = 1.75$ phase except for the cell parameters which are $a = 3.7962(1)$ Å and $c = 12.3892(3)$ Å.

The single phase $x = 1.75$ sample was used in the thermogravimetric, magnetic, and electrical transport studies. The thermogravimetric reduction plot is shown in Figure 4. The overall mass loss of 8.6(1)% agrees with the calculated loss of 8.5% expected for the hydrogen reduction of Ce(IV) and Ni(III) to Ce(III) and Ni metal. The derived composition of $Ce_{0.25}Sr_{1.75}NiO_{3.78(2)}$ is equivalent to $CeSr_7Ni_4O_{15.1(2)}$. The intermediate reduction stages are discussed below.

Figure 5 shows the molar susceptibility (χ_M) versus temperature plot for the $x = 1.75$ sample. The data are well-fitted by the equation $\chi_M = \chi_0 + C_M(T - \theta)^{-1}$ with the parameters shown in Table 3. The electrical resistivity of the $x = 1.75$ phase was found to show a metallic variation and is compared to that of the related phase $YSr_5Ni_3O_{11}$ in Figure 6.

Discussion

Quaternary oxides have not been previously reported in the $Ce_{2-x}Sr_xNiO_{4-\delta}$ or other Ce–Sr–Ni–O systems. The previously reported $Ln_{0.33}Sr_{1.67}NiO_{3.67}$ ($LnSr_5Ni_3O_{11}$) phases are stabilized by trivalent lanthanides for Ln = Nd–Tm[8,9] with (8-coordinate) ionic radii ranging between $r = 1.109$ and 0.994 Å.[13] (Yb, with $r = 0.985$ Å, forms an unrelated rhombohedral phase $YbSr_3NiO_6$.[14]) The Ce^{4+} ionic radius of 0.97 Å is comparable to the lower limit for the trivalent lanthanides, and so it is not surprising that the same structure type is adopted. The smaller Tb^{4+} ($r = 0.88$ Å) forms a mixture of phases including the perovskite $SrTbO_3$ under these conditions and no quaternary oxides are produced.[15]

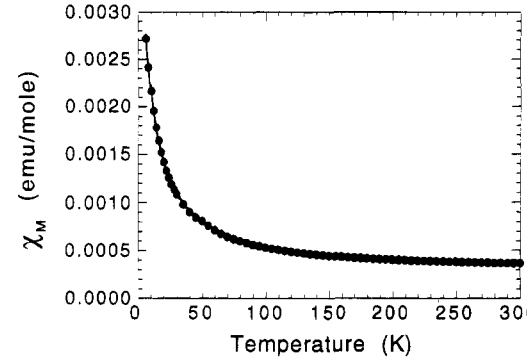

Figure 5. Molar susceptibility (χ_M) versus temperature for $Ce_{0.25}Sr_{1.75}NiO_{3.75}$.

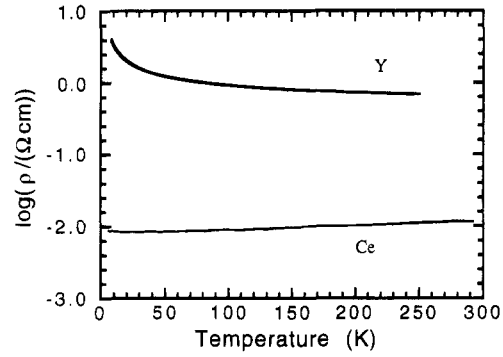

Figure 6. log(resistivity) versus temperature for $YSr_5Ni_3O_{11}$ (Y) and $CeSr_7Ni_4O_{15}$ (Ce).

Table 3. Parameters Derived by Fitting the Equation $\chi_M = \chi_0 + C_M(T - \theta)^{-1}$ to Magnetic Susceptibility Data for $Ce_{0.25}Sr_{1.75}NiO_{3.75}$ ($CeSr_7Ni_4O_{15}$) and $Ln_{0.33}Sr_{1.67}NiO_{3.67}$ ($LnSr_5Ni_3O_{11}$) with Ln = La and Y[6]

sample	χ_0 (emu/mol)	C_M (emu K/mol)	μ_{eff} (μ_B)[a]	θ (K)
$Ce_{0.25}Sr_{1.75}NiO_{3.75}$	0.0003	0.031	0.50	−6.2
$La_{0.33}Sr_{1.67}NiO_{3.67}$	0.0002	0.039	0.56	−10.8
$Y_{0.33}Sr_{1.67}NiO_{3.67}$	0.0002	0.039	0.56	−8.1

[a] $\mu_{eff} = 2.83\sqrt{C_M}$.

The observation that a single phase is produced for $Ce_{2-x}Sr_xNiO_{4-\delta}$ at the $x = 1.75$ composition but not for $x = 1.67$, supports the vacancy model discussed above. However, the cell parameters derived from the Rietveld refinement of the two structures do differ significantly, indicating a small range of solid solution around the ideal $x = 1.75$ composition.

The refined structure of $CeSr_7Ni_4O_{15}$ (Table 2) is similar to that of the previously reported $LnSr_5Ni_3O_{11}$ phases.[8,9] There is no evidence for any Ce/Sr ordering or deviation from tetragonal symmetry.

The TGA analysis confirms that the $x = 1.75$ phase is a stoichiometric Ce(IV)–Ni(III) oxide $CeSr_7Ni_4O_{15}$. The reduction profile shows three overlapping processes; an initial reduction to 95.2% at 550 °C, a more gradual

(14) James, M.; Attfield, J. P. *J. Mater. Chem.* **1994**, *4*, 575.

(15) Paletla, E.; Hoppe, R. *Naturwissenschaften* **1966**, *53*, 611.

decrease to 93.8% at 700 °C, and a rapid final reduction to 91.4% of the original mass at 780 °C. These correspond closely to the calculated masses after successive reduction of Ni(III) to Ni(I) (94.8%), Ce(IV) to Ce(III) (94.1%), and finally Ni(I) to Ni metal (91.5%). It is interesting to note that the reduction of Ni(III) to Ni(I) is almost complete before the reduction of Ce(IV) commences. Stable Ni(I) intermediates $LnSr_5Ni_3O_8$ (Ln = Y,[17] Dy–Tm[17]) have previously been isolated from the reduction of $LnSr_5Ni_3O_{11}$ phases.

The magnetic susceptibility variation and the derived parameters (Table 3) for $CeSr_7Ni_4O_{15}$ are very similar to those previously reported for the related Ni(III) phases $YSr_5Ni_3O_{11}$ and $LaSr_5Ni_3O_{11}$. The values of the temperature independent χ_0 term due to the contribution of ^4T excited states to the ^2E_g ground state are typical of Ni(III) oxides.[18] However, the values of C_M are consistently low in these materials, being only ~10% of the theoretical spin-only value of 0.374 emu K/mol for localized $S = 1/2$ Ni^{3+} ions. This reduction appears to be insensitive to the difference in overall electronic behavior between metallic $CeSr_7Ni_4O_{15}$ and semiconducting $YSr_5Ni_3O_{11}$. Strong antiferromagnetic correlations with $|J/k| \gg 300$ K could account for the reduced C_M values, although very strong exchange interactions would be needed to account for the good Curie–Weiss fit up to 300 K.

The metallic conductivity of $CeSr_7Ni_4O_{15}$ in Figure 6 is comparable to that of the isostructural, nondefective Ni(III) oxides $LnSrNiO_4$ where Ln = La[2] or Nd.[5] However, $YSr_5Ni_3O_{11}$ shows semiconducting behavior that is described by a 2-dimensional variable-range hopping model.[8] The difference in transport properties between these two materials is not due to a change in carrier concentration, as both are stoichiometric Ni(III) oxides, nor to geometric changes as the cell parameters and Ni–O bond distances in the two structures are very similar. The variation appears to be due to the difference in the concentration of O(1) oxygen vacancies which are formed in the NiO_2 planes. Ideally, 12.5% of the O(1) sites are vacant in $CeSr_7Ni_4O_{15}$ and 16.7% are vacant in $YSr_5Ni_3O_{11}$. Both values are much less than the percolation limit of 40% for a square lattice. The difference in electron mobility may instead be due to an Anderson transition,[19] as each random oxygen vacancy creates a large local potential. The increasing vacancy concentration causes the mobility edge to rise within the conduction band until it crosses the Fermi level, resulting in a change from metallic to insulating behavior. Further studies on $CeSr_7Ni_4O_{15}$–$YSr_5Ni_3O_{11}$ solid solutions are in progress to study the metal–insulator transition and unusual magnetic properties of these materials.

Conclusions

A new cerium(IV)–nickel(III) oxide $CeSr_7Ni_4O_{15}$ has been synthesized and characterized. Rietveld refinement using powder X-ray diffraction data show that this phase crystallises with the tetragonal K_2NiF_4 structure in space group *I4/mmm*. Susceptibility data show Curie–Weiss behavior in the range 6–300 K with a low value of the effective magnetic moment (0.50 μ_B per Ni^{3+} ion). $CeSr_7Ni_4O_{15}$ is a metallic conductor although the related phase $YSr_5Ni_3O_{11}$ is semiconducting. This difference may be due to an Anderson transition driven by the changing concentration of oxygen vacancies.

Acknowledgment. M.J. wishes to thank the University of Sydney and Newman College, Melbourne University for their financial support.

CM950290W

(16) James, M.; Attfield, J. P. *J. Chem. Soc., Chem. Commun.* **1994**, 1185.
(17) James, M.; Attfield, J. P. *Physica C* **1994**, *235–240* (II), 751.
(18) Byeon, S.-H.; Demazeau, G. *Mater. Lett.* **1991**, *12*, 158.
(19) Anderson, P. W. *Phys. Rev.* **1958**, *109*, 1492.